

**DESIGN AND SIMULATION OF RESONANT TUNNELING  
DIODE (RTD) BASED HIGH FREQUENCY MONOLITHIC  
MICROWAVE INTEGRATED CIRCUIT (MMIC)**

**CHIA YING YING**

**UNIVERSITI SAINS MALAYSIA**

**2018**

**DESIGN AND SIMULATION OF RESONANT TUNNELING  
DIODE (RTD) BASED HIGH FREQUENCY MONOLITHIC  
MICROWAVE INTEGRATED CIRCUIT (MMIC)**

**By**

**CHIA YING YING**

**This is submitted in partial fulfilment of the requirements for  
the degree of Bachelor of Engineering  
(Electronic Engineering)**

**JUNE 2018**

## **ACKNOWLEDGEMENTS**

First and foremost, I would like to express my sincere gratitude to my project's supervisor, Dr. Mohamad Adzhar Md Zawawi for the continuous support of this project. I really appreciate all the efforts, guidance, encouragement and helps given by him to complete my project with successful. His knowledge and advices are precious during the completion of my project. Again, I would like to thank you for his dedication and support in helping me in this project and also writing of thesis. I feel very grateful to have him as my supervisor throughout the project. Besides, I would like to thank to my examiner, Dr. Mohd Tafir Bin Mustaffa for his precious advices and efforts to support this project.

Apart from that, appreciations are dedicated to Pusat Pengajian Kejuruteraan Elektrik dan Elektronik (PPKEE) which provide the chance for undergraduates to gain engineering experience via the final year project (FYP). Through the course, some useful experiences were obtained which would be useful for undergraduate's future career development. Furthermore, the facilities available in PPKEE also helped a lot in completing this project smoothly.

In addition, I would like to extend my appreciation and gratefulness to my beloved family and friends. I am blessed with a lot of their full encouragement, moral support and understanding through all hardships along this project. So that I can accomplish this project with more efforts within the time given. Thank you for all supports.

# TABLE OF CONTENTS

|  |      |
|--|------|
| <b>ACKNOWLEDGEMENTS</b> .....                        | ii   |
| <b>TABLE OF CONTENTS</b> .....                       | iii  |
| <b>LIST OF TABLES</b> .....                          | vi   |
| <b>LIST OF FIGURES</b> .....                         | vii  |
| <b>LIST OF ABBREVIATIONS</b> .....                   | xi   |
| <b>ABSTRAK</b> .....                                 | xiii |
| <b>ABSTRACT</b> .....                                | xiv  |
| <b>CHAPTER 1 INTRODUCTION</b> .....                  | 1    |
| 1.1 Overview .....                                   | 1    |
| 1.2 Motivation .....                                 | 5    |
| 1.3 Problem Statement .....                          | 6    |
| 1.4 Objectives .....                                 | 7    |
| 1.5 Scopes of Research .....                         | 7    |
| 1.6 Thesis Outline .....                             | 8    |
| <b>CHAPTER 2 LITERATURE REVIEW</b> .....             | 9    |
| 2.1 Introduction .....                               | 9    |
| 2.2 Resonant Tunneling Diode (RTD): The Basics ..... | 9    |
| 2.2.1 RTD Double Barrier Quantum Well (DBQW) .....   | 10   |
| 2.2.2 Principle of RTD Operation .....               | 13   |
| 2.3 RTD Material System .....                        | 16   |
| 2.4 RTD: DC Characteristics .....                    | 18   |
| 2.4.1 Negative Differential Resistance (NDR) .....   | 19   |

|  |           |
|--|-----------|
| 2.5 Monolithic Microwave Integrated Circuit (MMIC) RTD oscillator design .....               | 20        |
| 2.5.1 Circuit Representation of RTD.....   | 20        |
| 2.5.2 Single RTD Oscillator Circuit.....   | 22        |
| 2.5.3 Double RTDs Oscillator Circuit.....  | 24        |
| 2.6 Summary .....  | 25        |
| <b>CHAPTER 3 METHODOLOGY.....</b>  | <b>26</b> |
| 3.1 Introduction.....  | 26        |
| 3.2 Introduction to LTspice XVII Software.....   | 29        |
| 3.3 Create New Library File for RTD Model .....  | 29        |
| 3.3.1 Create a circuit representation for RTD model .....                                    | 30        |
| 3.3.2 Choose one Analogue Behavioral Modelling to exploit I-V Characteristic of<br>RTD ..... | 31        |
| 3.3.3 Create a new symbol for RTD model.....   | 33        |
| 3.4 Design a MMIC oscillator circuit with appropriate value of passive components .....      | 33        |
| 3.4.1 Design a double RTDs oscillator using sample XMBE#66 GaAs/AlAs RTD .....               | 35        |
| 3.4.2 Design a double RTDs oscillator using sample XMBE#301 InGaAs/AlAs<br>RTD .....         | 38        |
| 3.5 Summary .....  | 39        |
| <b>CHAPTER 4 RESULTS AND DISCUSSION.....</b>   | <b>40</b> |
| 4.1 Introduction.....  | 40        |
| 4.2 GaAs/AlAs material system based RTD.....   | 40        |
| 4.2.1 Large Signal Model .....   | 40        |
| 4.2.2 Double RTDs in parallel configuration .....  | 46        |
| 4.3 InGaAs/AlAs material system based RTD .....  | 48        |
| 4.3.1 Large Signal Model .....   | 48        |
| 4.3.2 Double RTDs in parallel configuration .....  | 54        |

|  |           |
|--|-----------|
| 4.4 Comparison of both RTD oscillator made from different material system..... | 56        |
| 4.5 Summary .....  | 59        |
| <b>CHAPTER 5 CONCLUSION AND FUTURE WORK.....</b>                               | <b>60</b> |
| 5.1 Conclusion .....   | 60        |
| 5.2 Future Work.....   | 61        |
| <b>REFERENCES.....</b>   | <b>62</b> |
| <b>APPENDIX A: I-V Characteristic for XMBE#66 GaAs/AlAs RTD.....</b>           | <b>65</b> |
| <b>APPENDIX B: I-V Characteristic for XMBE#301 InGaAs/AlAs RTD .....</b>       | <b>67</b> |

## LIST OF TABLES

|   |    |
|---|----|
| Table 2.1: Sample XMBE#66 GaAs/AlAs RTD grown by MBE [4] .....  | 17 |
| Table 2.2: Sample XMBE#301 InGaAs/AlAs RTD grown by MBE [4] .....   | 18 |
| Table 4.1: Calculation of self-capacitance, $C_n$ for sample XMBE#66 GaAs/AlAs RTD. .   | 41 |
| Table 4.2: Calculation of series resistance, $R_s$ for sample XMBE#66 GaAs/AlAs RTD. ...  | 41 |
| Table 4.3: Comparison of device parameter between calculated and simulated value for<br>sample XMBE#66 GaAs/AlAs RTD model. ....                                      | 43 |
| Table 4.4: Parameter of DC characteristic for sample XMBE#66 GaAs/AlAs RTD model<br>with $C_n = 69.68\text{fF}$ and modified $R_s = 0.5\Omega$ .....                  | 45 |
| Table 4.5: The comparison of calculated and simulated results in terms of oscillating<br>frequency and RF output power for XMBE#66 GaAs/AlAs RTD oscillator. ....     | 47 |
| Table 4.6: Calculation of self-capacitance, $C_n$ for sample XMBE#301 InGaAs/AlAs<br>RTD.....   | 49 |
| Table 4.7: Calculation of series resistance, $R_s$ for sample XMBE#301 InGaAs/AlAs RTD.<br>.....  | 49 |
| Table 4.8: Comparison of device parameter between calculated and simulated value for<br>sample XMBE#301 InGaAs/AlAs RTD model. ....                                   | 51 |
| Table 4.9: Parameter of DC characteristic for sample XMBE#301 InGaAs/AlAs RTD<br>model with $C_n = 42.15\text{fF}$ and modified $R_s = 0.1\Omega$ .....               | 53 |
| Table 4.10: The comparison of calculated and simulated results in terms of oscillating<br>frequency and RF output power for XMBE#301 InGaAs/AlAs RTD oscillator. .... | 55 |
| Table 4.11: Comparison of final results of MMIC oscillator using RTDs made from<br>samples XMBE#66 GaAs/AlAs and XMBE#301 InGaAs/AlAs.....                            | 56 |

## LIST OF FIGURES

|   |    |
|---|----|
| Figure 1.1: Frequency and wavelength spectra of electromagnetic waves [1].  | 1  |
| Figure 1.2: Basic Structure of Double Barrier RTD based on experimental GaAs/AlAs material system [6].  | 3  |
| Figure 1.3: Typical Current-Voltage (I-V) characteristic of RTD (solid line) and conventional p-n diode (dashed line) [6].  | 3  |
| Figure 2.1: Schematic layer structure of RTD device using InGaAs/AlAs material system which is employed in this project [1].  | 11 |
| Figure 2.2: Schematic conduction band diagram of a double barrier quantum well (DBQW) RTD device. $E_{fL}$ and $E_{fR}$ denote the Fermi level of the left and right contact layer. $E_{r1}$ and $E_{r2}$ denote the quantized resonant state in the quantum well [1].  | 12 |
| Figure 2.3: Electron particle-wave duality (quantum tunneling) in (a) classical view and (b) quantum mechanical view [4].   | 13 |
| Figure 2.4: Conduction band diagram of a DBQW structure forming the RTD at different forward bias voltage ( $V_b$ ) conditions with respective I-V characteristic: (a) no bias (b) positive bias applied to the emitter in forward bias condition at threshold voltage (c) forward bias at peak voltage (resonant tunneling) (d) NDR region showing decreasing tunneling current and (e) forward bias above valley voltage (non-resonant energy). $E_{fL}, E$ and $E_{fR}, C$ are the Fermi level of left emitter layer and right collector layer respectively. $E_{cL}, E$ and $E_{cR}, C$ are the conduction band edge of the emitter and collector. $E_{r1}$ and $E_{r2}$ represent the resonant energy state in the quantum well [6]. | 15 |
| Figure 2.5: Example of an I-V characteristic with NDR region from an RTD fabricated using sample XMBE#230 [4].  | 18 |
| Figure 2.6: Circuit representation for RTD model. (a) Large signal model. (b) Small signal model [24].  | 20 |

|  |    |
|--|----|
| Figure 2.7: (a) Single RTD oscillator topology with shunt resistor $R_e$ and decoupling capacitor $C_e$ . (b) Large signal model. RTD is represented by its self-capacitance, $C_n$ in parallel with voltage controlled current source, $i(v)$ . (c) Small signal equivalent circuit. RTD is represented by its self-capacitance, $C_n$ in parallel with the negative conductance, $-G_n$ [1]. ..... | 22 |
| Figure 2.8: (a) Two RTDs oscillator circuit topology with its own DC stabilization circuit, $R_e$ and $C_e$ . Two RTD devices are employed in parallel with each device is biased individually. (b) Small signal equivalent circuit. ....  | 24 |
| Figure 3.1: Flowchart of project: (a) Steps in creating RTD library files. (b) Application of RTD in MMIC oscillator circuit. ....   | 28 |
| Figure 3.2: Circuit Symbol for Voltage Dependent Current Source, $G$ . ....  | 30 |
| Figure 3.3: Circuit Symbol for Independent Current Source, $I_1$ . ....  | 31 |
| Figure 3.4: Example of look -up table method for Independent Current Source, $I_1$ used in this project. ....  | 32 |
| Figure 3.5: Circuit Symbol for RTD.....  | 33 |
| Figure 3.6: Double RTDs oscillator circuit designed using LTspice. ....  | 34 |
| Figure 3.7: Simplified small signal equivalent circuit of the double RTDs oscillator employing two RTD devices.....  | 34 |
| Figure 4.1: Circuit representation of RTD model with $C_n = 69.68\text{fF}$ and $R_s = 1.5\Omega$ . ....   | 41 |
| Figure 4.2: New symbol created for sample XMBE#66 GaAs/AlAs RTD model.....   | 42 |
| Figure 4.3: Circuit diagram in simulation of I-V characteristic for sample XMBE#66 GaAs/AlAs RTD model. ....   | 42 |
| Figure 4.4: Comparison of measured and simulated result for I-V curve of sample XMBE#66 GaAs/AlAs RTD model with $R_s = 1.5\Omega$ and $C_n = 69.68\text{fF}$ .....  | 43 |

|  |    |
|--|----|
| Figure 4.5: Circuit representation of RTD with $C_n = 69.68\text{fF}$ and modified $R_s = 0.5\Omega$ . ....  | 44 |
| Figure 4.6: Comparison of measured and simulated result for I-V curve for sample XMBE#66 GaAs/AlAs RTD model with $C_n = 69.68\text{fF}$ and $R_s = 0.5\Omega$ . ....  | 44 |
| Figure 4.7: LTspice schematic of the RTD oscillator circuit employing two RTDs made from sample XMBE#66 GaAs/AlAs. ....  | 46 |
| Figure 4.8: Time domain signal of output voltage across load resistor, $R_L$ with oscillating frequency of 65.39 GHz when $V_{\text{bias}} = 0.45\text{V}$ and $I_{\text{bias}} = 40.96\text{mA}$ . ....   | 46 |
| Figure 4.9: Simulated spectrum of a double RTD oscillator using sample XMBE#66 RTDs with fundamental oscillations at 65.39GHz with $0.774\mu\text{W}(-31.11\text{dBm})$ output power when $V_{\text{bias}} = 0.45\text{V}$ and $I_{\text{bias}} = 40.96\text{mA}$ . .... | 47 |
| Figure 4.10: Circuit representation of RTD model with $C_n = 42.15\text{fF}$ and $R_s = 3.375\Omega$ . ....  | 49 |
| Figure 4.11: New symbol created for sample XMBE#301 InGaAs/AlAs RTD model. ....  | 50 |
| Figure 4.12: Circuit diagram in simulation of I-V characteristic for sample XMBE#301 InGaAs/AlAs RTD model. ....   | 50 |
| Figure 4.13: Comparison of measured and simulated result for I-V curve of sample XMBE#301 InGaAs/AlAs RTD model with $C_n = 42.15\text{fF}$ and $R_s = 3.375\Omega$ . ....   | 51 |
| Figure 4.14: Circuit representation of RTD with $C_n = 42.15\text{fF}$ and modified $R_s = 0.1\Omega$ . ..   | 52 |
| Figure 4.15: Comparison of measured and simulated result for I-V curve for sample XMBE#301 InGaAs/AlAs RTD model with $C_n = 42.15\text{fF}$ and modified $R_s = 0.1\Omega$ . .  | 52 |
| Figure 4.16: LTspice schematic of the RTD oscillator circuit employing two RTDs made from sample XMBE#301 InGaAs/AlAs. ....  | 54 |
| Figure 4.17: Time domain signal of output voltage across load resistor, $R_L$ with oscillating frequency of 114GHz when $V_{\text{bias}} = 0.39\text{V}$ and $I_{\text{bias}} = 85.66\text{mA}$ . ....   | 54 |

Figure 4.18: Simulated spectrum of a double RTD oscillator using sample XMBE#301  
RTDs with fundamental oscillations at 114GHz with 4.601 $\mu$ W(-23.37dBm) output  
power when Vbias = 0.39V and Ibias = 85.66mA. ....55

## LIST OF ABBREVIATIONS

|               |  |
|---------------|--|
| <b>AC</b>     | Alternating Current                      |
| <b>Al</b>     | Aluminium                                |
| <b>AlAs</b>   | Aluminium Arsenide                       |
| <b>AlGaAs</b> | Aluminium Gallium Arsenide               |
| <b>As</b>     | Arsenide                                 |
| <b>CMOS</b>   | Complementary Metal Oxide Semiconductor  |
| <b>DBQW</b>   | Double Barrier Quantum Well              |
| <b>DC</b>     | Direct Current                           |
| <b>Ga</b>     | Gallium                                  |
| <b>GaAs</b>   | Gallium Arsenide                         |
| <b>GHz</b>    | Gigahertz                                |
| <b>In</b>     | Indium                                   |
| <b>InAlAs</b> | Indium Aluminium Arsenide                |
| <b>InAs</b>   | Indium Arsenide                          |
| <b>InGaAs</b> | Indium Gallium Arsenide                  |
| <b>InP</b>    | Indium Phosphide                         |
| <b>IMPATT</b> | Impact Ionization Avalanche Transit-time |
| <b>MBE</b>    | Molecular Beam Epitaxy                   |
| <b>MHz</b>    | Megahertz                                |
| <b>MMIC</b>   | Monolithic Microwave Integrated Circuit  |
| <b>NDR</b>    | Negative Differential Resistance         |

|                |                                  |
|----------------|----------------------------------|
| <b>PDR</b>     | Positive Differential Resistance |
| <b>PVCR</b>    | Peak-to-Valley Current Ratio     |
| <b>QW</b>      | Quantum Well                     |
| <b>RF</b>      | Radio Frequency                  |
| <b>RTD</b>     | Resonant Tunneling Diode         |
| <b>Si</b>      | Silicon                          |
| <b>THz</b>     | Terahertz                        |
| <b>TUNNETT</b> | Tunneling Transit-time           |

## ABSTRAK

Diod terowong resonan (RTD) dianggap sebagai peranti elektronik berasaskan semikonduktor terpanas sehingga sekarang. Mereka berpotensi untuk direalisasikan pada frekuensi terahertz (THz) yang beroperasi pada suhu bilik berdasarkan sifat uniknya terhadap rintangan negatif (NDR). Walaupun begitu, batasan utama pengayun berasaskan RTD sehingga kini adalah kuasa outputnya yang rendah disebabkan oleh ayunan bias parasit dan dimensi peranti yang kecil. Oleh itu, tesis ini telah membuktikan satu siri litar bersepadu gelombang mikro monolitik (MMIC) bagi pengayun berasaskan model RTD yang sesuai. Matlamat akhir kerja ini adalah untuk mewujudkan model RTD yang optimum untuk dilaksana ke dalam pengayun RTD litar bersepadu gelombang mikro monolitik (MMIC) yang berfrekuensi tinggi.

Model RTD dicipta dengan bahan yang berbeza berdasarkan hubungan arus dan voltan (I-V) dengan beberapa parameter DC penting seperti ketumpatan arus puncak ( $I_p$ ), voltan puncak ( $V_p$ ) dan nisbah arus antara puncak dengan lembah (PVCR). Peranti RTD terdiri daripada lapisan jurang jalur yang sempit yang diapit di daerah pemisah yang tipis (DBQW). Apabila peranti itu berada dalam kondisi bias maju, elektron dengan tenaga kinetik yang lebih rendah daripada DBQW itu boleh menembusi celah pemisah tersebut. Peranti itu akan mempamerkan karakteristik kerintangan negatif (NDR) yang wujud dalam hubungan I-V. Properti ini sangat penting dalam pelaksanaan litar kerana ia dapat mengawal voltan dalam keadaan logik yang berbeza dan bersamaan dengan arus puncak dan lembah. Oleh itu, pelbagai lengkungan hubungan I-V yang sesuai digunakan untuk peranti RTD telah dimodelkan supaya ia dapat dipasang dalam litar pengayun dengan tepat.

Dalam projek ini, salah satu cabaran adalah untuk menangani batasan kuasa output pengayun RTD yang rendah. Oleh itu, dalam kerja ini, satu siri litar bersepadu gelombang mikro monolitik (MMIC) dengan diod terowong resonan (RTD) telah dibentangkan. Salah satu topologi litar pengayun ialah menggunakan dua peranti RTD secara selari. Manakala setiap peranti adalah dibias secara individu. Berbanding dengan pengayun RTD tunggal, dua RTD telah digabungkan pada tahap litar untuk memaksimumkan kuasa output. Kerja ini menunjukkan potensi pengayun RTD sebagai sumber terahertz (THz) untuk pelbagai aplikasi termasuk komunikasi tanpa wayar yang berkelajuan tinggi.

## ABSTRACT

Resonant tunneling diodes (RTD) are considered as the fastest semiconductor-based electronic devices demonstrated to date. They are promising for realizing a terahertz (THz) sources operating at room temperature by virtue of its unique characteristic of negative differential resistance (NDR). However, the main limitation of RTD based oscillators up to now is their low output power due to parasitic bias oscillations and small device dimensions. Hence, this paper has demonstrated a series of monolithic microwave integrated circuit (MMIC) oscillators with the appropriate RTD models created. The final aim of this work was to create an optimized RTD model to be implemented into MMIC RTD oscillators.

The RTD model was created using different material systems based on current-voltage (I-V) characteristic with some important DC parameters such as peak current density,  $I_p$ , peak voltage,  $V_p$  and peak-to-valley-current ratio (PVCr). The RTD device consists of a narrow bandgap layer (quantum well) sandwiched between two thin wide bandgap layers (barriers). When the RTD is biased, electrons with kinetic energy lower than the barriers may tunnel through the double barrier quantum well (DBQW) structure, and the device will exhibit a negative differential resistance (NDR) in I-V curve. This property is very essential in the circuit application because it can provide for the different voltage-controlled logic states corresponding to the peak and valley currents. So, a well-suited range of I-V curve was modelled for RTD device so that it can be fitted in oscillator circuit accurately.

In this project, one of the challenges was to solve the limitations of low output power of RTD oscillators. Thus, in this work, a series of monolithic microwave integrated circuit (MMIC) RTD oscillators has been presented. One of the oscillator circuit topologies is by applying two RTD devices in parallel. While each device is biased separately. Compared with single RTD oscillators, double RTDs oscillator can maximize the output power. This work proves the promising potential of RTD device in MMIC oscillators as Terahertz (THz) sources for a variety of applications especially high-speed wireless communication.

# CHAPTER 1

## INTRODUCTION

### 1.1 Overview

Terahertz (THz) is generally defined as the electromagnetic radiation with frequencies located in the region between 0.3 THz to 3 THz in the electromagnetic spectrum which in between microwave and infrared with their corresponding wavelength ( $\lambda$ ) from 1mm to 100 $\mu$ m as shown in Figure 1.1 below [1]. This THz technology is attracting more and more research interest because of its potential for the use in new high-frequency applications. For example, radio astronomy, medical imaging, security imaging, ultra-broadband wireless communication and so on [2].

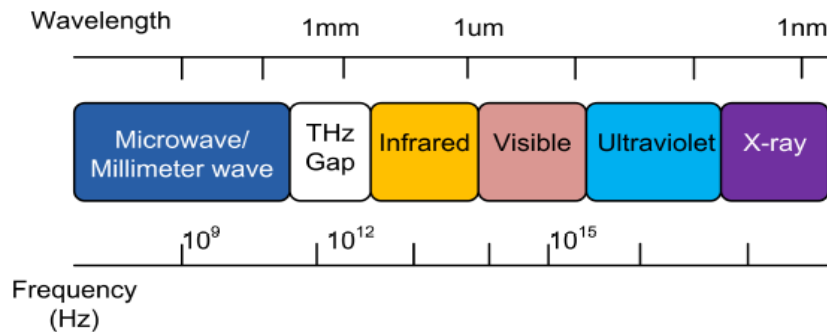


Figure 1.1: Frequency and wavelength spectra of electromagnetic waves [1].

As the demand for high speed wireless communication increases, compact and room temperature operation terahertz (THz) transmitters and highly sensitive detectors are required. Since the THz range is located between light waves and millimeter waves, both optical and electronic devices are being investigated for THz sources. For semiconductor single oscillators, both p-type germanium lasers and recently developed THz quantum cascade lasers are studied from the optical device side. From the electron device side, few electronic devices may also be applied to build THz sources. These include the development of two-terminal devices such as impact ionization avalanche transit-time (IMPATT) diodes, tunneling transit-time (TUNNETT) diodes, Gunn diodes, and resonant tunneling diodes (RTDs) [3].

However, among these devices, RTDs exhibit the highest oscillating frequency. The resonant tunneling diode (RTD) device is one of the promising technology platforms and candidate for electronic THz communications. In fact, conventional transistor technology will not be able to support future ultra-high speed, high frequency applications, especially when it comes to sub-THz or THz frequencies at room temperature because of the extremely scaled device geometries required ( $< 10\text{nm}$ ) which lead to problems like leakage currents, parasitics and device fragility (breakdown  $< 0.5\text{V}$ ) [4]. So, RTDs have been widely investigated for their importance in realizing very high speed in wide-band devices and circuits application that are beyond conventional transistor technology.

RTDs have started to receive a lot of attention following the pioneering work by Esaki and Tsu over the past three decades in 70' [4]. In comparison with conventional diode, RTD device is an attractive device, not only because it provides an insight into quantum mechanics theory, but also it shows negative differential resistance (NDR) from DC up to THz. This makes RTDs as the fastest solid state electronic devices demonstrated to date. Hence, it has the ability to generate continuous-wave terahertz frequency at room temperature. Until now, the highest room temperature fundamental oscillation of up to 1.31 THz was reported in thin-well RTD made of InGaAs/AlAs. This work was demonstrated by Professor Masahiro Asada from Tokyo Institute of Technology [5].

Resonant tunneling diodes (RTDs) consists of a narrow band gap layer (quantum well) sandwiched in between two thin wide band gap layers (barriers). Due to the different bandgaps of these two semiconductor materials, a double barrier quantum well (DBQW) is formed. The electrons will be able to penetrate through the DBQW due to the tunneling effect at specific bias voltage given. While the operating principle of tunneling that based on resonant tunneling effect in finite semiconductor superlattices was first proposed by Tsu and Esaki in 1973. They observed resonant energies in electron tunneling within an experimental AlAs/GaAs/AlAs double-barrier heterostructure as illustrated in Figure 1.2 in which the bias dependence of the tunneling current through the structure results in negative difference resistance (NDR) [6] .

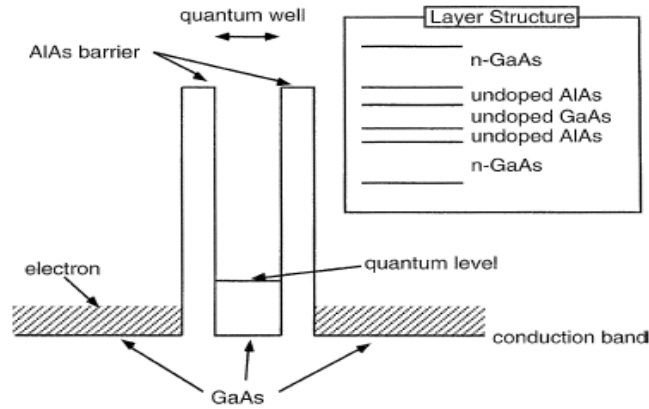


Figure 1.2: Basic Structure of Double Barrier RTD based on experimental GaAs/AlAs material system [6].

Following Esaki's discovery, the resonant tunneling diode (RTD) is also a two-terminal non-linear device with an N-shaped current-voltage (I-V) characteristic showing peak current,  $I_p$  at resonant energies. The I-V curve exhibits one or more NDR regions which enable RTD to be used in a sustained oscillator. Figure 1.3 below shows the typical I-V characteristic of a RTD (solid line) along with the I-V characteristic of a conventional p-n junction diode (dashed line) showing the peak and valley current points,  $I_p$  and  $I_v$ , the peak and valley voltage points,  $V_p$  and  $V_v$ , and NDR region. The peak-to-valley current and voltage differences are denoted by  $\Delta I$  and  $\Delta V$ .

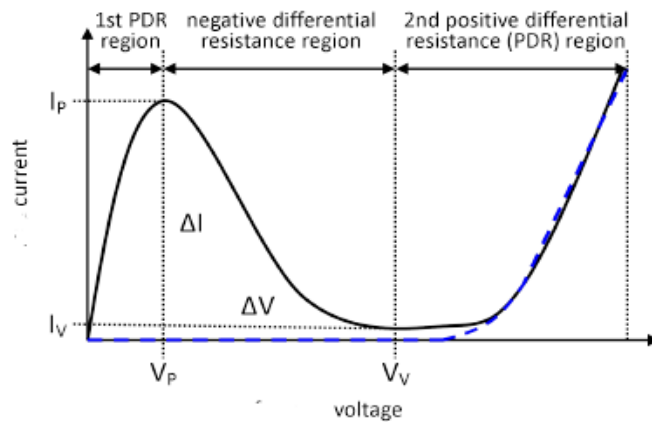


Figure 1.3: Typical Current-Voltage (I-V) characteristic of RTD (solid line) and conventional p-n diode (dashed line) [6].

According to I-V curve shown, three main regions will be referred which are the first positive differential resistance (PDR), the NDR and the second PDR regions. From a circuit design point of view, an attractive and potentially useful feature of RTDs is its NDR region [7]. Negative resistance is the most important element to prevent an oscillation from damping to build a sustained oscillator. Although the NDR region in RTD device is the reason they are well-suited to oscillator realization, however, due to the DC instability, low frequency parasitic oscillations and underdeveloped circuit design techniques, the output power of RTD oscillators tends to be low. This has become the limitation of RTD oscillator up to now. The highest frequency of single RTD oscillator published is 1.4 THz, of which the output power is just  $1\mu\text{W}$  [8].

Presently, far-infra-red lasers, backward-wave oscillators (BWOs), or Gunn oscillator-varactor multiplier combinations are implemented at THz frequencies, for instance, a 580 GHz radar with a multiplier based LO of 0.3 to 0.4 mW output power was recently demonstrated for imaging applications [9] and a 420 GHz radar for sensing and imaging of biological materials and agents in the range of 1 km requires 1 mW output power [10]. These examples are exactly in the range in which the RTD oscillator would be competitive because of its low power requirements and the portable compact sources that could be achieved. However, RTD oscillators providing such output powers are yet to be developed [8]. To address the limitation of lower output power of RTD oscillator circuit, a new multiple device circuit topology for oscillator must be developed.

In this paper, the library file of the RTDs will be created using LTspice software since it does not provide the built-in model for RTDs. Two basic RTD models will be developed from two different material systems made of III-V compound semiconductor. The first type is Indium Gallium Arsenide/Aluminium Arsenide (InGaAs/AlAs) material system while the second type is Gallium Arsenide/Aluminium Arsenide (GaAs/AlAs) material system. Semiconductor InGaAs or GaAs quantum well is sandwiched in between the two layers of AlAs barriers. Their corresponding current-voltage (I-V) relationship will be observed and compared with the experimental result obtained from previous work by Md Zamawi et. al [4]. Each RTD model is then being applied and simulated in a high frequency oscillator

circuit. This paper has presented a series of monolithic microwave integrated circuit (MMIC) oscillator. But the oscillator circuit topology based on the power combining technique will be used by employing two RTDs in parallel configuration in order to maximize the output power. Finally, the results from the oscillator circuit will be analyzed in term of oscillating frequency and output power for each RTD model applied. In overall, this work will show the promising potential of RTDs in achieving ultrahigh speed oscillator with high output power.

## **1.2 Motivation**

Till now, there is an increasing number of applications that require signal source at very high frequencies starting from 300Hz until around 1.5THz. Obviously, there are many present and future applications of terahertz technology. Historically, the microelectronics industry has scaled down CMOS transistor dimensions to increase operating speeds and decrease cost per transistor. Yet, there is still a limitation on the recent trend of scaling down the transistors and integrated circuits in order to achieve faster speeds and lower power consumption due to large channel doping, short gate lengths, and very thin gate oxides. The highest frequency of conventional transistor oscillator built today is only about 215Hz [11].

However, tunnel diodes (TD) are being investigated as a CMOS augmentation technology. They have been shown to exhibit fast switching speeds, thereby increasing the operating frequency that circuits may be operated at [11]. Resonant tunneling diode (RTD) is currently fast device which able to operate up to 1.31THz in room temperature for future high-frequency applications. With this remarkable high-speed performance, RTD has wide variety of applications for microwave and millimeter wave oscillation circuits. RTDs exhibit negative differential resistance (NDR) characteristic which is important in building a sustained oscillation. So, RTDs can be deeply studied and improved to exploit NDR of the devices current-voltage (I-V) characteristic for the well-known purposes: the development of THz sources [12]. It also gives us motivation in doing more research on output power of RTD oscillator circuit and integrate them with conventional transistor.

### 1.3 Problem Statement

As mentioned, resonant tunneling diode (RTD) devices exhibit negative differential resistance (NDR) in I-V characteristics which extends from DC up to terahertz (THz). This feature makes the RTD a very promising device to realize compact, room temperature operating terahertz sources. In previous researches, experiment was carried out to investigate the DC characteristic from I-V characteristics of the RTD device before continuing researches on the application of RTD device in oscillator circuit.

In this project, LTspice software will be used to implement RTD device into oscillator circuit for analyzing purpose. However, the problem is that this software does not include a built-in model for an RTD device. There are various methods that can be used to create a suitable RTD model. By using the analogue behavioral modeling, a compatible RTD model can be created in its equivalent circuit and exploit its current-voltage (I-V) characteristics with negative differential resistance (NDR) region [13].

However, the main parameter that researched focused on is not only the oscillating frequency but also output power. Up to date, the biggest limitation of RTD oscillators is low output power [1]. About thirty years ago, Brown et. al has presented a fundamental frequency of 712 GHz. It has been the highest frequency ever achieved till 2012 when Feiginov et al. reported their work in which 1.11 THz with a very low output power of  $1\mu\text{W}$ . On year 2012, Teranishi et al. make another record of 1.08 THz with an improved output power of  $5.5\mu\text{W}$ . For the published RTD oscillators, the output power is only in the range of micro-Watts ( $\mu\text{W}$ ) [11].

From the point of view of the oscillating frequency, RTDs have shown their potential in reaching the sub-THz and THz region. Yet more problems were found in achieving a good power level. The reasons for the very low output power of the RTD-based oscillators include the low-frequency parasitic bias oscillations and the inefficient oscillator circuit topologies [14]. A series of MMIC RTD oscillator circuit have been developed but oscillator with power combining technique is applied to maximize the output power.

## **1.4 Objectives**

To investigate the potential of RTDs in improving the oscillating frequency and output power for high frequency MMIC oscillator, a research with the following objectives is carried out.

- a. To design a library file for resonant tunneling diode (RTD) based on I-V characteristics.
- b. To design a high frequency oscillation circuit which is Monolithic Microwave Integrated Circuit (MMIC) oscillator.
- c. To investigate the performance of created RTD model in the MMIC oscillator.

## **1.5 Scopes of Research**

This research will focus on the study of fastest device with high oscillating frequency in Terahertz (THz) technology which is resonant tunneling diode (RTD). Analogue structural modelling will be applied to obtain a compatible model for RTD in LTspice software. They will be mainly made from InGaAs/AlAs and GaAs/AlAs material system with different current-voltage (I-V) characteristics. The I-V characteristics will be simulated and compared with the experimental I-V curve from previous work [4]. The DC parameters such as peak current density,  $J_p$ , peak voltage,  $V_p$  as well as the peak-to-valley current ratio (PVCR) will be determined from I-V curve.

After that, a monolithic microwave integrated circuit (MMIC) oscillator circuit with power combining techniques will be demonstrated with the purpose of solving the bottleneck of RTD oscillator which are low output power at millimeter-wave or even higher frequencies. This new created RTD models will be applied and simulated in the MMIC double RTD oscillator. The theory of operation for RTD oscillators will be studied and described. Besides that, oscillation frequency and output power will be analyzed theoretically and experimentally.

## **1.6 Thesis Outline**

The present thesis is divided into five chapters which are organized as following:

Chapter 1 describes the background information and the importance of the work. The problem statement and objectives of carrying out this project and the scope of research are also included.

Chapter 2 discuss some basic understanding of resonant tunneling diode (RTD) based on double barrier quantum well (DBQW) and its epitaxy layer structure. Thereafter, the basic operation of RTD is presented. This chapter also covers properties and characteristics of materials from III-V compound semiconductors which are used to created RTD model. The RTD DC characteristic are listed towards the last part of Chapter 2. The equivalent circuit for RTD will be presented. Lastly, a series of MMIC RTD oscillator will be introduced with some necessary equations needed for analyze purpose.

Chapter 3 describes the methodology that has been carried out in this research. It involves the steps in creating an RTD model in LTspice and also steps in designing a MMIC oscillator circuit. The process and the circuitry used in this research are further explained in detail in this chapter.

Chapter 4 shows the results obtained from this research. It covers the simulation of RTD library file and also application of RTD model into oscillator circuit. The results obtained are compared with the theoretical values. A discussion is made in this chapter to justify the difference between the RTD material used and their effect to the results in term of oscillating frequency and output power. The results are analyzed and discussed in this chapter.

Finally, Chapter 5 concludes the research. Further improvement and suggestion about this research are proposed.

## **CHAPTER 2**

### **LITERATURE REVIEW**

#### **2.1 Introduction**

This chapter is devised to cover few important aspects which are related to work on design and simulation of resonant tunneling diode (RTD) on high frequency microwave monolithic integrated circuit (MMIC) oscillator. First of all, the basic structure of the resonant tunneling diodes (RTDs) device which corresponds to double barrier quantum well (DBQW) is discussed. Secondly, an in-depth description is presented into the basic operation of RTD including quantum tunneling and effect of bias voltage to DBQW. Next, important structural parameters and material system for RTD will be explained. This work will mainly focus on InGaAs/AlAs and GaAs/AlAs material system. An introduction to RTD high frequency capability will be discussed in terms of its principles and unique device characteristic, which is the negative differential resistance (NDR). Finally, small equivalent circuit of RTD model is introduced. A series of MMIC RTD oscillator circuit is presented to show the promising potential of high-frequency RTD in high-speed application.

#### **2.2 Resonant Tunneling Diode (RTD): The Basics**

Unlike the bipolar Esaki tunnel diodes, resonant tunneling diodes (RTDs) utilize only electrons (most common) or holes. RTD is a two-terminal device which operates on the principle of electron tunneling. It is a heterostructure. A heterostructure is a device having a combination of heterojunctions, and the heterojunction is a junction formed between two dissimilar layers having unequal energy band gaps. It is usually manufactured using molecular beam epitaxy (MBE) [6].

RTD is a semiconductor device in which its peculiar epitaxial structure creates, in the conduction band, a finite potential well buried between two thin finite potential barriers. This system is named as Double Barrier Quantum Well (DBQW) in which there is a wide bandgap material forms two tunneling barriers in between a narrow bandgap material to forms a quantum well. The electrons able to penetrate through the DBQW using tunneling effect

which occurs at certain bias voltages. However, the quantum well will allow only a limited number of discrete energies (quantization) for the moving particles.

RTDs are capable of ultra-high-speed operations as the quantum tunneling effect through the very thin layers is a very fast process. Its current-voltage (I-V) characteristic also exhibits negative differential resistance (NDR) region. Hence, RTDs provide an insight into quantum mechanics theory and show broadband NDR from DC up to terahertz (THz) which makes it a very promising electronic device for THz applications [12].

### **2.2.1 RTD Double Barrier Quantum Well (DBQW)**

A mentioned, RTD in its most common form, is a two-terminal electronic device that consists of a undoped quantum well sandwiched between two undoped layers of barriers. This basic RTD device configuration is so called Double-Barrier Quantum Well (DBQW) structure. DBQW is the conventional, most common RTD structures as described by Sun et. al [15] and of relevance to this project. This DBQW RTD was first experimentally demonstrated by Chang et. al [16].

RTD consists of three parts. The first part is an emitter region which is the source of electrons. The second part is a double-barrier quantum-well (DBQW) structure which consists of a narrow band-gap quantum-well material sandwiched between two barriers of wide band-gap material. The third part is a collector region to collect the electrons tunneling through the double-barrier structure [14]. The quantum well and the two barriers are located between two heavily-doped n-type materials with small band gaps which form the emitter and collector regions.

Figure 2.1 shows an example of schematic layer structure for RTD with DBQW which is studied in this project. We can see that RTD is formed as a single compressively strained quantum well structure (InGaAs) sandwiched between two very thin tensile strained barrier layers (AlAs). The other layers are InGaAs lattice-matched to InP semi-insulating substrate. Because of the difference of these two semiconductor material bandgaps, a DBQW is formed.

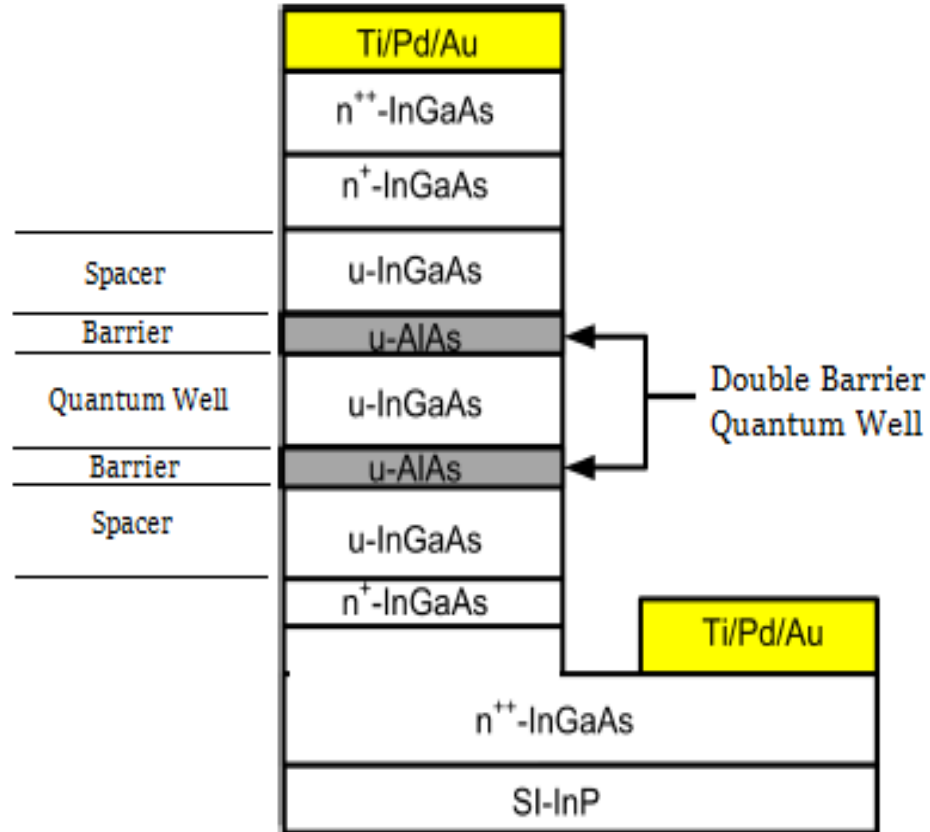


Figure 2.1: Schematic layer structure of RTD device using InGaAs/AlAs material system which is employed in this project [1].

According to Figure 2.1, it is noted that the basic structure and materials used to form the RTDs are mostly from compound semiconductors of group III-V. Main reasons for the use of these materials are due to the ability to design the band-gaps of these materials to improve electron mobility, hence higher current density capability. The fact that these materials can be highly doped contributes to their popularity among the RTD community. The group III-V material systems are normally grown on GaAs substrates. For this GaAs substrate, the cladding layers and the quantum well would be made of GaAs while the barrier would be made of lattice-matched  $\text{Al}_x\text{Ga}_{1-x}\text{As}$  or very slightly strained AlAs [4]. Beside these, there are some other material systems being used for producing RTDs with improvements on the DC characteristics such as peak current density,  $J_p$ , peak voltage,  $V_p$ , peak to valley current ratio (PVCR) and the negative differential resistance (NDR). Some of these materials will be discussed in the next sections.

The band diagram of the DBQW in InGaAs/AlAs material system is shown in Figure 2.2. There are several quantized energy states ( $E_{r1}$  and  $E_{r2}$ ) existing in the well according to quantum mechanical theory. The term “resonant” in the name of resonant tunneling diode refers to the behaviour of electrons with kinetic energy lower than that the barrier potential but that still be able to travel though the double barriers. The possibility of electrons tunneling through the barriers is defined by the transmission coefficient. At the resonant state, the transmission coefficient is close to unity. As the transmission coefficient of electrons tunneling through the DBQW changes with the bias voltage, the current-voltage (I-V) characteristic of resonant tunneling devices exhibits negative differential resistance (NDR).

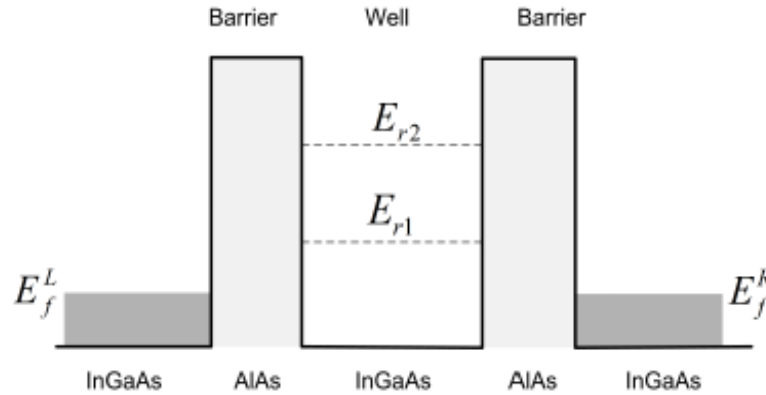


Figure 2.2: Schematic conduction band diagram of a double barrier quantum well (DBQW) RTD device.  $E_f^L$  and  $E_f^R$  denote the Fermi level of the left and right contact layer.  $E_{r1}$  and  $E_{r2}$  denote the quantized resonant state in the quantum well [1].

Hence, due to the reason of the characteristic dimensions of the DBQW structure is comparable with the electron wavelengths, the wave nature of electrons leads to quantum phenomena, for example, interference, tunneling, energy quantization and so forth [15]. As a result, resonant tunneling phenomena occur in DBQW structures and form the basis for RTD operation.

### 2.2.2 Principle of RTD Operation

Quantum mechanics is a very powerful theory which stipulates that in contrast to classical belief, solid particles have wave-like properties. A RTD makes use of a process called quantum mechanical tunneling, in which electrons can tunnel through some resonant states at certain energy levels. Quantum tunneling is mainly an effect when electrons pass through a barrier which is sufficiently thin compared to the electron wavelength. However, there is a possibility that the wave appears on both sides of the barrier when the “electron wave” is large enough compared to the barrier.

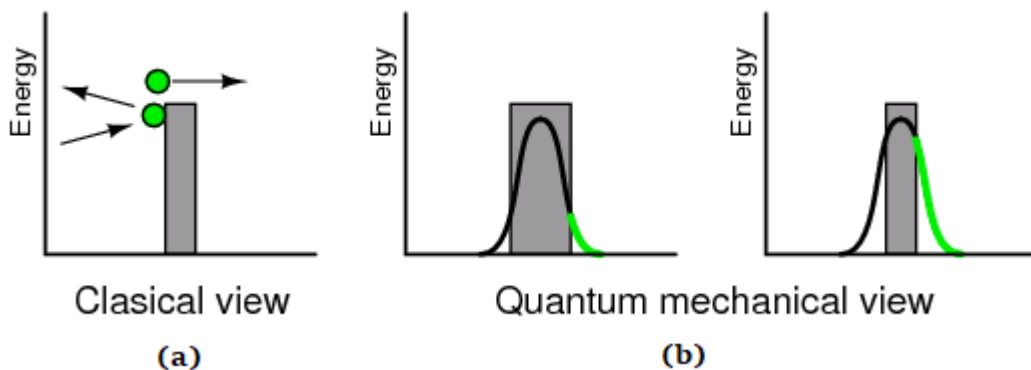


Figure 2.3: Electron particle-wave duality (quantum tunneling) in (a) classical view and (b) quantum mechanical view [4].

In classical physics, an electron must sustain enough energy to surmount a barrier. Or else, it will rebound from the barrier as shown in Figure 2.3(a) above. While for quantum mechanics, it only allows a probability for electrons being in the other side of the barrier as illustrated in Figure 2.3(b). If served as a wave, the electron may look larger compared to barrier thickness. Even if the electron is treated as a wave, there is still a small probability that it will appear on the other side of a thick barrier (refer to green portion of curve in Figure 2.3(b)). Particle with incident energy less than the barrier height can tunnel through the barrier and appears on the other side of the barrier with certain probabilities, which are improved when the barrier is thin enough and finite [4].

Generally, tunneling mechanisms in semiconductor devices are categorized into two major types. The first one is the interband tunneling where electrons tunnel from conduction band to valence band or holes tunneling from valence band to conduction band. This mechanism needs bipolar device with p-type and n-type doping. The second type is the intraband tunneling in which electrons tunnel from conduction band to conduction band or holes tunnel from valence band to valence band. In these cases, devices are needed to be unipolar, either n-doped or p-doped. This intraband tunneling device will be focused this work since RTD is a unipolar device.

The conduction band diagram of the double barrier RTD structure at different states of forward bias is presented in Figure 2.4. When no bias voltage is applied, no current is observed due to thermal equilibrium as seen in Figure 2.4(a). When a bias voltage is applied and increased, the first resonant energy level,  $E_{r1}$  is moved to the Fermi energy level,  $E_{F,E}$  in the conduction band as can be seen in Figure 2.4(b). More electrons obtain kinetic energy under an electric field and tunnel through the barrier, leading to an increased current. When the energy of electrons corresponding to the increased bias voltage matches the conduction band at the energy level,  $E_{C,E}$  as in Figure 2.4(c), the resonant energy state is reached and the transmission coefficient is unity. It means large amounts of electrons will tunnel through the DBQW structure without being rejected. The peak tunneling current,  $I_p$  is achieved in the I-V plot. With further increase of the bias voltage, the first resonant energy level,  $E_{r1}$  is lowered below the emitter conduction band,  $E_{C,E}$  as shown in Figure 2.4(d) which is turning off the electron available for tunneling through barrier. Fewer electrons can go through the barrier and so the current starts to decrease creating a negative differential resistance (NDR) region between peak voltage,  $V_p$  and valley voltage,  $V_v$ . In Figure 2.4(e), when a larger bias voltage is further applied, the second energy level,  $E_{r2}$  is moved to the emitter conduction band,  $E_{C,E}$  which enables a second tunneling process. Here, thermionic emission of electrons contributes to most of the current, so the thermionic current increases with the bias proportionally [6].

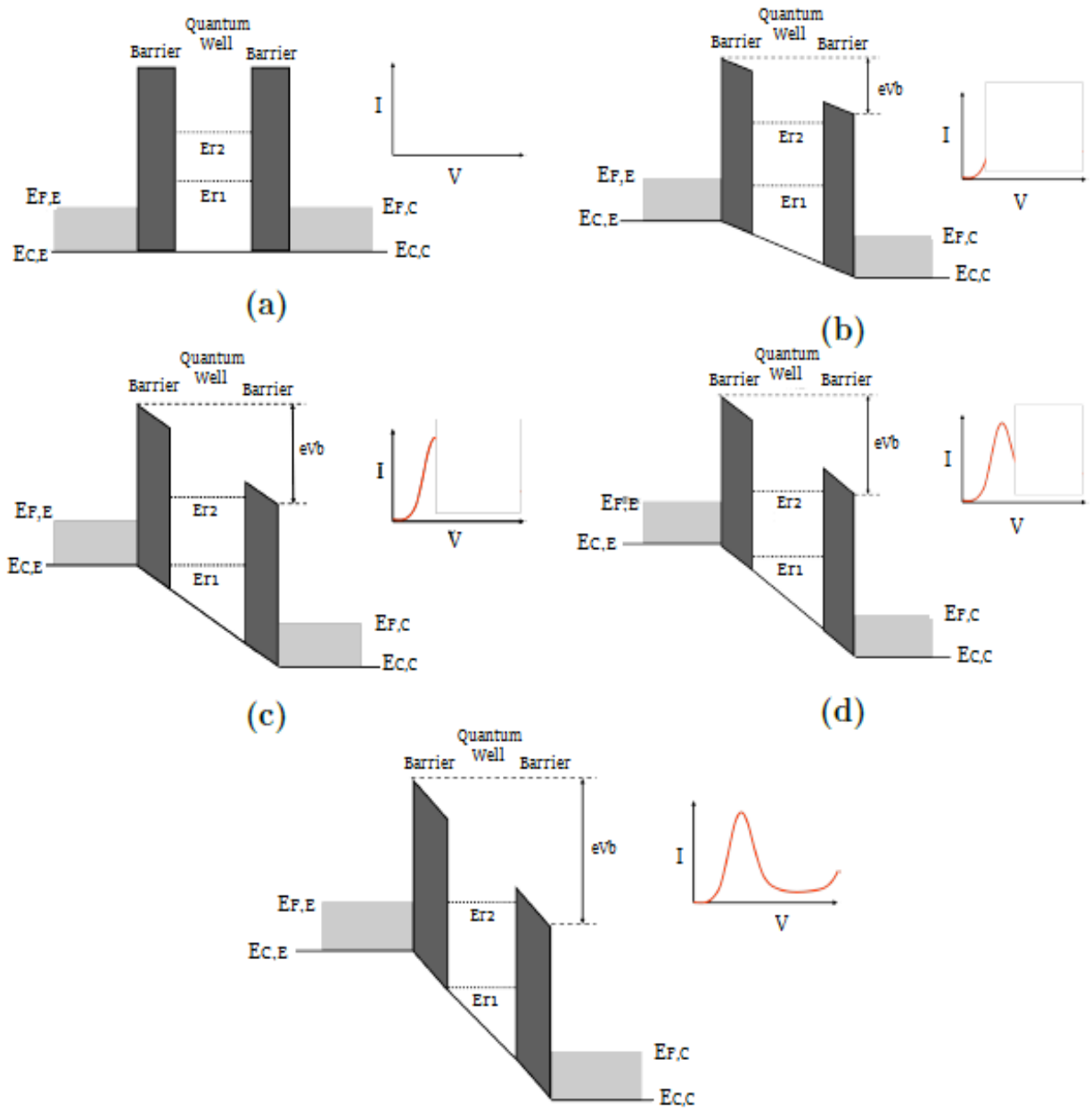


Figure 2.4: Conduction band diagram of a DBQW structure forming the RTD at different forward bias voltage ( $V_b$ ) conditions with respective I-V characteristic: (a) no bias (b) positive bias applied to the emitter in forward bias condition at threshold voltage (c) forward bias at peak voltage (resonant tunneling) (d) NDR region showing decreasing tunneling current and (e) forward bias above valley voltage (non-resonant energy).  $E_{F,E}$  and  $E_{F,C}$  are the Fermi level of left emitter layer and right collector layer respectively.  $E_{C,E}$  and  $E_{C,C}$  are the conduction band edge of the emitter and collector.  $Er_1$  and  $Er_2$  represent the resonant energy state in the quantum well [6].

### 2.3 RTD Material System

The performance of a double barrier quantum well RTD can be maximized through proper selection of material system. Traditionally, RTDs were made using III-V semiconductors due their mature growth technique and excellent properties of the materials. Especially the ability to adjust the band-gap of the materials to produce higher electron mobility through reduction in electron effective mass. There are several material systems being used for the fabrication of double barrier structures with improvements on the DC characteristics namely the peak current density,  $J_p$ , peak voltage,  $V_p$ , peak-to-valley current ratio (PVCR) and negative differential resistance (NDR).

The most common RTD material system which can be used to fabricate RTDs includes GaAs/AlGaAs, GaAs/AlAs, InGaAs/InAlAs, InGaAs/InAlAs, InGaAs/AlAs and InAs/AlSb. However, the material system used in this research are InGaAs/AlAs and GaAs/AlAs which mainly focuses on the comparison between the wider peak-to-valley current ratio (PVCR) with the smallest PVCR. Here, the properties of these two material systems will be presented but the fabrication process of double barrier structures for RTD will not be discussed in this project.

**GaAs/AlAs material system:** Resonant tunneling diodes with GaAs/AlAs material system had been introduced for the first time by Tsuchiya et. al in 1985 [17]. The electrodes were highly doped and NDR at room temperature was observed. In 1990, the highest ever reported peak current density,  $J_p$  was demonstrated by Wolak et. al with an impressive  $200 \text{ kA/cm}^2$  [18]. Apart from that, the highest reported peak-to-valley current ratio (PVCR) for this material system was presented by Forster et. al in 1993 with 5.35 obtained with optimization done through growth temperature at  $580 \text{ }^\circ\text{C}$  [19]. Generally, improvement of  $J_p$  was due to increase in transmission probability. The improvement in PVCR were attributed by reducing alloy scattering in the binary AlAs barrier which lead to reduction in leakage current components and decrease in leakage through the higher lying resonant level due to the increased barrier height.

**InGaAs/AlAs material system:** RTD with InGaAs/AlAs material system had been introduced by Inata et. al in 1987 in order to improve peak current density as well as PVCR by increasing barrier even higher. Initially, Inata et. Al obtained a high PVCR of 14 [20]. Broekeart et. al obtained a higher PVCR of 23 in 1988 [21]. In 1995, the highest peak current density of  $680\text{kA/cm}^2$  was reported by Shimizu et.al [22]. The aim of this work is to produce RTD oscillator with highest frequency. With this quantum well made of InGaAs/AlAs material system, RTD oscillator with terahertz and sub-terahertz can be achieved since it has higher PVCR compared to GaAs/AlAs based RTD. To date, the highest ever 1.31 THz oscillator at room temperature has been reported by Asada et. al in 2012 using this structure [5].

Semiconductor film growth has benefited from modern epitaxial layer growth techniques such as molecular beam epitaxy (MBE). This technique provides high quality semiconductor materials growth with precise composition and thickness control. In 2015, eight different samples of RTD devices which were made from III-V material systems were grown and fabricated using MBE by Md Zamawi et. al [4]. The eight different samples used to fabricate RTD device included XMBE#66, XMBE#230, XMBE#276, XMBE#277, XMBE#301, XMBE#302, XMBE#308 and XMBE#327. In my work, sample XMBE#66 GaAs/AlAs and sample XMBE#301 InGaAs/AlAs are chosen to be the active RTD component mainly for realization of high frequency MMIC oscillator. Table 2.1 and Table 2.2 below demonstrate these two samples of RTD structures used in this work [4].

Table 2.1: Sample XMBE#66 GaAs/AlAs RTD grown by MBE [4]

| Layer        | Material  | Doping ( $\text{cm}^{-3}$ ) | Thickness ( $\text{\AA}$ ) |
|--------------|-----------|-----------------------------|----------------------------|
| Collector    | GaAs(n++) | $7.0 \times 10^{18}$        | 5000                       |
| Spacer       | GaAs      | undoped                     | 150                        |
| Barrier      | AlAs      | undoped                     | 17                         |
| Quantum Well | GaAs      | undoped                     | 65                         |
| Barrier      | AlAs      | undoped                     | 17                         |
| Spacer       | GaAs      | undoped                     | 350                        |
| Emitter      | GaAs(n++) | $3.0 \times 10^{18}$        | 8000                       |
| Buffer       | GaAs      | undoped                     | 1320                       |
| Substrate    | GaAs      |                             |                            |

Table 2.2: Sample XMBE#301 InGaAs/AlAs RTD grown by MBE [4]

| Layer        | Material                                      | Doping (cm <sup>-3</sup> ) | Thickness (Å) |
|--------------|---|----------------------------|---------------|
| Collector 1  | In <sub>0.53</sub> Ga <sub>0.47</sub> As(n++) | 2.0 × 10 <sup>19</sup>     | 450           |
| Collector 2  | In <sub>0.53</sub> Ga <sub>0.47</sub> As(n+)  | 3.0 × 10 <sup>18</sup>     | 250           |
| Spacer       | In <sub>0.53</sub> Ga <sub>0.47</sub> As      | undoped                    | 200           |
| Barrier      | AlAs  | undoped                    | 11            |
| Quantum Well | In <sub>0.8</sub> Ga <sub>0.2</sub> As        | undoped                    | 45            |
| Barrier      | AlAs  | undoped                    | 11            |
| Spacer       | In <sub>0.53</sub> Ga <sub>0.47</sub> As      | undoped                    | 200           |
| Emitter 2    | In <sub>0.53</sub> Ga <sub>0.47</sub> As(n+)  | 3.0 × 10 <sup>18</sup>     | 250           |
| Emitter 1    | In <sub>0.53</sub> Ga <sub>0.47</sub> As(n+)  | 1.0 × 10 <sup>19</sup>     | 4000          |
| Substrate    | InP   |                            |               |

## 2.4 RTD: DC Characteristics

The tunneling effects in semiconductor leads to a phenomenon called the negative differential resistance (NDR). This was first suggested by Tsu and Esaki in 1973 [14]. NDR is a circuit element with the property of decreasing current with increasing voltage. Figure 2.5 shows a typical I-V characteristic of an RTD fabricated from the work of Md Zamawi et. al [4] using sample XMBE#230 In<sub>0.8</sub>Ga<sub>0.2</sub>As/AlAs which shows a clear NDR region.

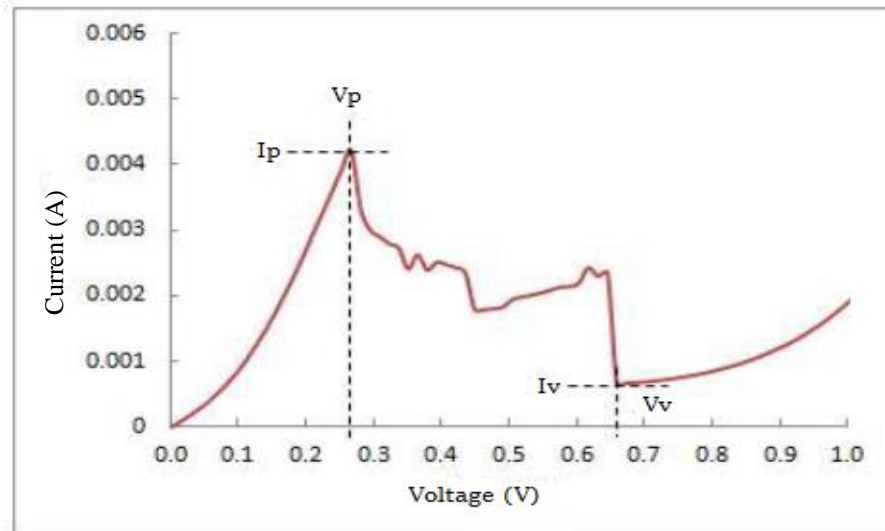


Figure 2.5: Example of an I-V characteristic with NDR region from an RTD fabricated using sample XMBE#230 [4].

### 2.4.1 Negative Differential Resistance (NDR)

The most important property of an RTD lies in its NDR, which ensures a sustainable oscillator in high frequency and offers very fast switching speed. The NDR is a phenomenon happening in RTD when the electrons pass through the barrier by tunneling process. Figure 2.5 shows the actual I-V characteristics for positive polarity. Compared to Figure 1.3, the I-V curve shows a plateau-like feature in the NDR region. There is a sudden drop of current flow at about 0.65 V. This is caused by low frequency bias oscillation.

NDR is happening in the region between peak current,  $I_p$  and valley current,  $I_v$ . So, the peak-to-valley current ratio (PVCR) is an important parameter of RTDs. To achieve the maximum dynamic range, the I-V curve in the negative resistance voltage range should be very sharp resulting in a high PVCR [23]. For high frequency operation, very high peak current densities are needed to obtain the maximum power available for RTD. Hence, the peak current,  $I_p$  must be as large as possible while the valley current,  $I_v$  must be as small as possible in order to have large PVCR ideally according to the Equation 2.1 below.

$$PVCR = \frac{I_p}{I_v} \quad (2.1)$$

Nonetheless, too large peak current ( $I_p$ ) may raise the problem of high power dissipation. To reduce power dissipation of the diode when it is “on”, a low peak voltage,  $V_p$  of RTD can be designed in this paper.

The negative differential conductance,  $G_n$  can provide the gain necessary to sustain an RTD oscillation.

$$G_n = \frac{1}{R_n} = \left| \frac{I_p - I_v}{V_p - V_v} \right| \quad (2.2)$$

## 2.5 Monolithic Microwave Integrated Circuit (MMIC) RTD oscillator design

The term oscillator is used to describe a circuit which will produce a continuing, repeated waveform without input other than perhaps a trigger. There are many ways in producing oscillator circuit. While in my work, a designed RTD model will be applied in a high frequency oscillator circuit - Monolithic Microwave Integrated Circuit (MMIC) oscillator. A MMIC is a type of integrated circuit (IC) device that operates at microwave frequencies in between 300 MHz and 300 GHz. Normally, oscillator has its own electrical resistance, so the oscillation will be damped at the end. With implementation of RTD device in oscillator, its negative differential resistance (NDR) characteristic will cancel off the positive internal loss resistance to create a continuous and sustained oscillation at its resonant frequency. Previous researches have been done and a series of MMIC RTD oscillator circuit topologies will be introduced with the discussion about its frequency bias oscillation and the output power. Before we look into the MMIC RTD oscillator design, the circuit representation for RTD model will be discussed before it is implemented into the oscillator.

### 2.5.1 Circuit Representation of RTD

Basically, in large signal model of circuit representation, an RTD device can be modeled by a voltage-controlled current source  $I(V)$  in parallel with the self-capacitance,  $C_n$  together with the series resistance,  $R_s$  as illustrated in Figure 2.6(a) below. The self-capacitance,  $C_n$  is the RTD device's capacitance resulting from charging and discharging of the double barrier quantum well (DBQW) and the depletion region. While the series resistance,  $R_s$  is connected arising from the ohmic contact and the resistivity of the emitter and collector region of RTD since the device is not ideal.

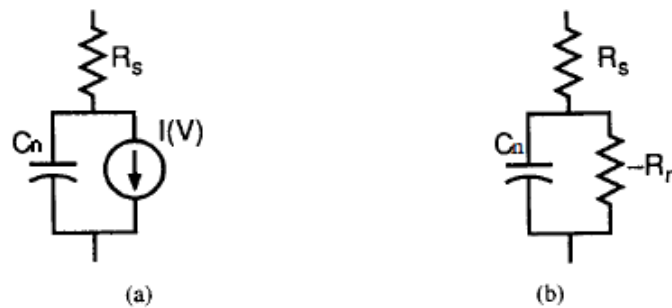


Figure 2.6: Circuit representation for RTD model. (a) Large signal model. (b) Small signal model [24].

Since the double barrier quantum well (DBQW) structure of RTD is an undoped region sandwiched between two heavily doped contact regions, the device capacitance,  $C_n$  can be hence given approximately by:

$$C_n = \frac{A\epsilon_0\epsilon_r}{d} \quad (2.3)$$

where,  $\epsilon_0$  is the permittivity of free space,  $\epsilon_r$  is the relative permittivity of the barrier and well materials,  $A$  is the mesa area of the RTD device while the thickness of the DBQW structure is denoted by  $d$  in which consists of the width of the barrier layers, the quantum well and any spacer layers [14].

The series resistance,  $R_s$  can be given by the simple equation as below:

$$R_s = \frac{R_o}{A} \quad (2.4)$$

$R_o$  is the characteristic resistance of the parasitic layer structure in which  $R_o = \sim 54\Omega \mu\text{m}^2$  while  $A$  is the mesa area of RTD device [25].

It is noted that the current,  $I(V)$  is replaced by the negative differential resistance,  $-R_n$  in the small-signal model as seen in Figure 2.6(b). It represents the corresponding negative differential conductance,  $-G_d$  where the relationship between  $R_d$  and  $G_d$  has been shown in the Equation 2.2. In this work, different approaches can be applied for voltage-controlled current source,  $I(V)$  in order to describe the I-V characteristic of RTD model which will be discussed in next Chapter 3.

### 2.5.2 Single RTD Oscillator Circuit

From the I-V measurement data shown in Figure 2.5, a plateau-like current distortion is observed in the NDR region between peak voltage,  $V_p$  and valley voltage,  $V_v$ . This is because of the presence of the low frequency bias oscillation, which reduces the RF output power at the design frequency. Therefore, to suppress the bias oscillation, the strategy adopted is to employ a shunt resistor,  $R_e$ .

Figure 2.7(a) below illustrates an example for single MMIC RTD oscillator circuit.  $V_{bias}$  is the bias voltage to set the device in the NDR region.  $R_b$  and  $L_b$  are the resistance and inductance introduced by the connecting cable. The shunt resistor,  $R_e$  is employed to suppress the low-frequency bias oscillation, and  $C_e$  is the decoupling capacitor acting as the RF short to the ground to avoid the RF power being dissipated by the shunt resistor,  $R_e$ .

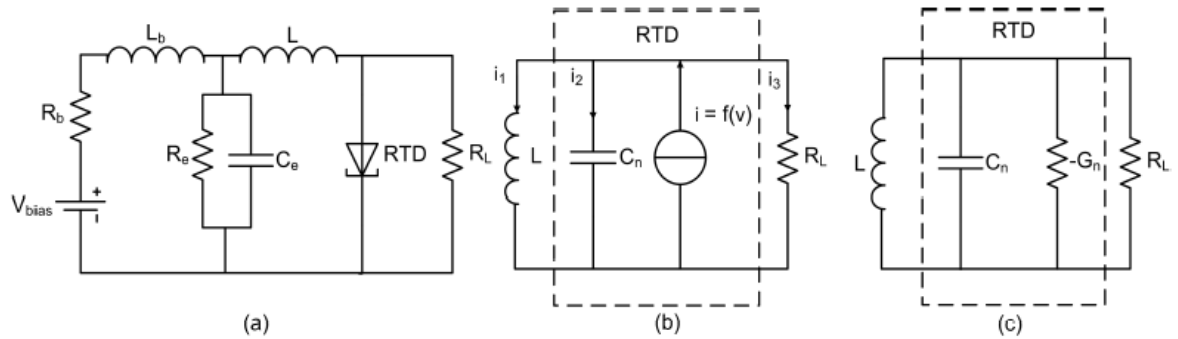


Figure 2.7: (a) Single RTD oscillator topology with shunt resistor  $R_e$  and decoupling capacitor  $C_e$ . (b) Large signal model. RTD is represented by its self-capacitance,  $C_n$  in parallel with voltage controlled current source,  $i(v)$ . (c) Small signal equivalent circuit. RTD is represented by its self-capacitance,  $C_n$  in parallel with the negative conductance,  $-G_n$  [1].

For the circuit to be DC stable in which the low frequency bias oscillations are suppressed, previous studies have derived and proved that the value of  $R_e$  should satisfy the criteria as shown below [1][14]:

$$R_e < R_n = \frac{1}{G_n} \quad (2.5)$$

Since the maximum value of the negative conductance,  $G_{n(\max)}$  is located at the middle of the NDR region with its value:

$$G_{n(\max)} = \frac{3\Delta I}{2\Delta V} \quad (2.6)$$

By rearranging the Equation 2.5:

$$Re < \frac{1}{G_{n(\max)}} \quad (2.7)$$

$$Re < \frac{2\Delta V}{3\Delta I} \quad (2.8)$$

Hence, Equation 2.8 must be applied to obtain an approximate Re value which is low enough to achieve bias stability but high enough to minimize the DC power dissipation in Re itself.

Finally, the small signal equivalent circuit of the single RTD oscillator is shown in Figure 2.7(c). The very small value of series resistance,  $R_s$  in the small signal model has been ignored in the following analysis due to the undoped region of RTD device. The frequency of the oscillation,  $f_{osc}$  can be obtained as below [1]:

$$f_{osc} = \frac{1}{2\pi\sqrt{LC_n}} \quad (2.9)$$

The theoretical maximum RF power of a single RTD device can be estimated from the I-V characteristic using equation below [1]:

$$\text{RF power, } P_{RF} = \frac{3}{16} (\Delta I \times \Delta V) \quad (2.10)$$

where  $\Delta I = I_p - I_v$  and  $\Delta V = V_p - V_v$ .

Equation 2.10 provides an estimation of the expected maximum RF output power that can be generated by a MMIC RTD oscillator. To obtain a large RF power, the  $\Delta I$  and  $\Delta V$  must be made as large as possible. However, in practical RTD oscillator circuit implementation, actual output RF power will be much more less due to the imperfection from the effect of parasitic resistance and impedance mismatched.

However, this circuit with only one RTD will give out a low output power due to the its difficulty to employ large size RTD device without bias oscillation. As a proof, the output power of the single RTD oscillator operating at a record of high frequency 1.1THz is only  $0.1\mu\text{W}$  [26].

### 2.5.3 Double RTDs Oscillator Circuit

As for the single RTD oscillator, the output power is very small. The oscillator circuit topology utilizing two RTDs was proposed as shown in Figure 2.8(a). Each device of RTD1 and RTD2, is biased individually with a separate stabilizing circuit. Each RTD device has its own DC stabilization circuit which are  $R_{e1}$ ,  $R_{e2}$ ,  $C_{e1}$  and  $C_{e2}$ . While the small signal equivalent circuit for the two RTD oscillator is shown in Figure 2.8(b).  $-G_{1n}$  and  $-G_{2n}$  are the negative differential conductance whereas  $C_{1n}$  and  $C_{2n}$  are the capacitances of the RTD1 and RTD2 biased in the its NDR region respectively.

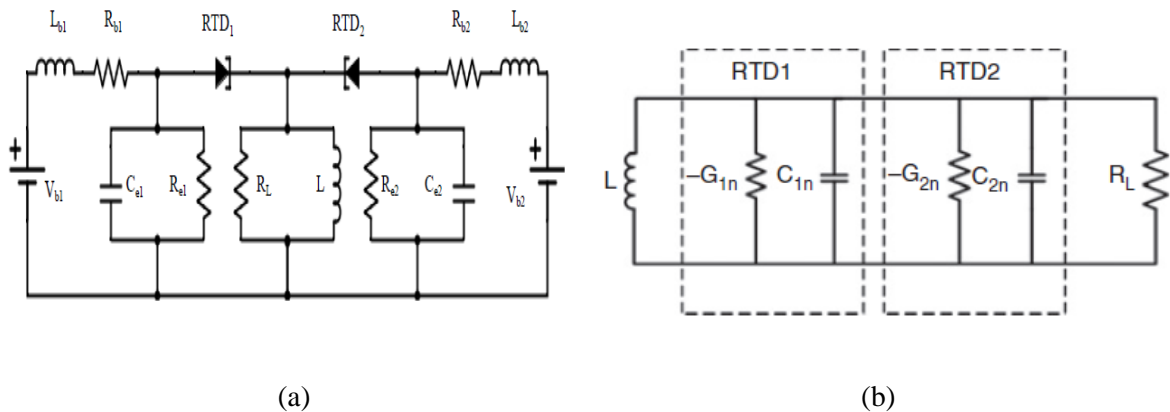


Figure 2.8: (a) Two RTDs oscillator circuit topology with its own DC stabilization circuit,  $R_e$  and  $C_e$ . Two RTD devices are employed in parallel with each device is biased individually. (b) Small signal equivalent circuit.